Modeling Framework for Dynamic Wing Loads and Control Design of a Flexible Aircraft

Modeling Framework for Dynamic Wing Loads and Control Design of a Flexible Aircraft

Simone Malisani* and Elisa Capello†
Politecnico di Torino, Torino, Italy, 10129

A framework for dynamic load evaluation of low-order model of a flexible aircraft is proposed. A mixed Newtonian-Lagrangian approach for the longitudinal model definition is derived. The key feature of the proposed approach is the design of a computational efficient model, suitable for synthesizing active control techniques. The main objectives are: (1) definition of a low computational model and (2) design of a control system, able to alleviate the dynamic loads when a disturbance occurs. An $\mathcal{L}_1$ adaptive controller is proposed for the alleviation of gust dynamic loads in the framework of flexible fixed wing subsonic aircraft. Numerical results show the effectiveness of the proposed control system. A comparison with a Linear Quadratic Regulator is also proposed.

I. Introduction

Due to progress in aerospace materials and on optimised structural designs, more light and slender aircraft structures are designed, to obtain weight, drag reduction and, consequently, more efficient aircraft in terms of fuel consumption. However, these slender structures tend to be highly deformable, and thus the assumption of rigid body is no longer acceptable [1]. Moreover, the deformation of the structure increases fatigue loads by means of dynamic loads generated by maneuvers and/or by external perturbations. Finally, more flexibility leads to lower frequencies of the structural modes which might couple with typical aircraft dynamics frequencies [2] resulting in dangerous resonance phenomenons.

Flexible aircraft models have been a subject of study not only in recent years, but comprehensive mathematical formulations of the problem have been derived for both structural dynamics [3] and aeroelastic [4] purposes. Nevertheless, these formulations are usually not suitable for real-time applications because of their high complexity level. First flexible aircraft models have been studied starting from the early 1960s. At that time strong simplifications were required to find equations solutions, because of the lack of computational power. The work of Milne [5] is an example, in which small deformations were considered for the aircraft longitudinal motion.

In 2004, Meirovitch and Tuzcu [6] presented a model based on Lagrange's equations but without the need to determine the mean axes position. Their approach consists in deriving an hybrid system of ordinary and partial differential equations in terms of quasi-coordinates (or generalized coordinates), which permits to express the transport degrees of freedom in terms of flight variables, as linear and angular velocities. This is convenient for real time simulation of the flexible structure but compromises the simplicity of the formulation, since the Lagrange's equation has to take in consideration additional terms and, also, the obtained hybrid system of ordinary and partial equations needs some form of discretization.

Avanzini *et.al.* [7] proposed a minimum-complexity flexible model, which includes the effects of bending and torsion of fuselage and wings on the aircraft rigid dynamics. In [7] classical equations of flight dynamics are derived the rigid degrees of freedom and the Lagrange's equations are considered for the flexible terms. The method proposed in this paper is based on [7], even if only the wing is considered as deformable system. An extension of the method in [7] is the definition of the dynamics loads, responsible of fatigue increase and performance reduction. The main objectives of this approach are: (i) definition of a low order model for wing dynamic loads, including flexible effects, and (ii) a computational efficient algorithm, combined with a control system synthesize, to improve the overall flight dynamics. Even if this modeling framework introduces some simplifications, it is particularly convenient for real time simulations and for the design of control laws, with interactions between structure dynamics, flight mechanics and control. The application of an $\mathcal{L}_1$ adaptive controller is shown to alleviate the dynamic loads, when a gust occurs. As detailed in [8–10], this adaptive controller is capable of compensating for unexpected events, without a gain scheduling of the

*Graduate Research Fellow, Department of Mechanical and Aerospace Engineering, Politecnico di Torino, Corso Duca degli Abruzzi 24, Torino, 10129, Italy

†Assistant Professor, Department of Mechanical and Aerospace Engineering, Politecnico di Torino, CNR-IEIIT, Corso Duca degli Abruzzi 24, Torino, 10129, Italy

control parameters. A comparison with a Linear Quadratic Regulator is also proposed, to show the performance of the adaptive controller, when parametric uncertainties and different gusts are considered.

The paper is organized as follows. The rigid and flexible mathematical model is described in Section II, in which the gust models and the linearized equations of motion are included. Section III introduces two methods for the wing load evaluation. In Section IV both the proposed controllers are presented. Simulation results with different gust inputs and variations of aircraft parameters are in Section V. Finally, conclusions are drawn in Section VI

II. Mathematical Modelling

Since the model is based on a mixed Newtonian-Lagrangian approach, as described in [6, 7], the formulation can be divided in two main sections: rigid aircraft dynamics and flexible structural dynamics.

Moreover, a section concerning the atmospheric turbulence is included, in which the gust is considered as perturbation in the rigid equations of motion. Two gust models are tested in this study: (i) a continuous gust model, based on von Karman turbulence as in [11, 12], and (ii) a discrete gust model, according to the relevant EASA certification (paragraph CS 25.341 of [13]) and as described in [11].

The mathematical model is summarized in Fig. 1.

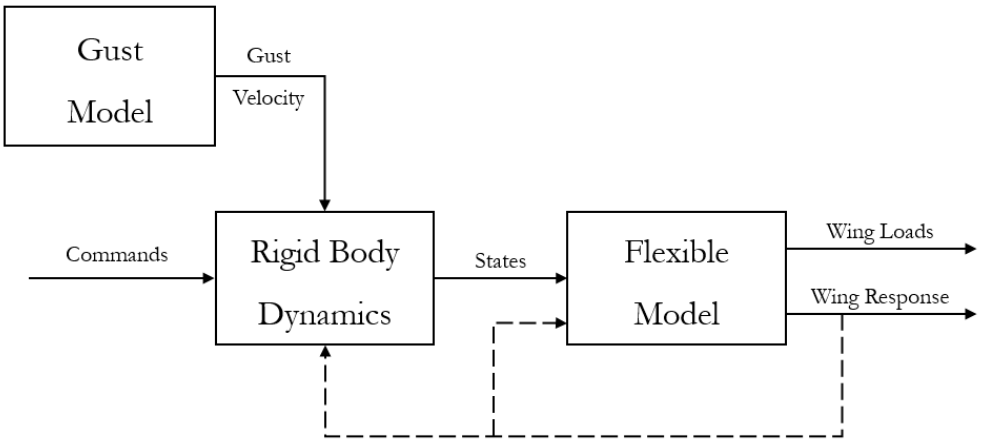

Fig. 1 Mathematical Model Scheme

A. Rigid Aircraft Dynamics

The rigid model is based on nonlinear equations of motion, written in body frame as in [14]. The resulting 6 Degree-of-Freedom (DoF) differential equation system includes 12 variables: linear velocities $U = [u, v, w]^T \in \mathbb{R}^3$, angular rates $\omega = [p, q, r]^T \in \mathbb{R}^3$, Euler angles $\Phi = [\phi, \theta, \psi]^T \in \mathbb{R}^3$ (order of rotation: 3-2-1) and, finally, coordinates $\mathrm{X} = [\mathrm{x_N}, \mathrm{y_E}, \mathrm{z_D}]^{\mathrm{T}} \in \mathbb{R}^3$ in North-East-Down (NED) reference frame.

As well known, force equations are classically expressed directly in terms of linear accelerations, as reported in the following matrix form

$$\begin{Bmatrix} \dot{u} \\ \dot{v} \\ \dot{w} \end{Bmatrix} = -\begin{bmatrix} 0 & -r & q \\ r & 0 & -p \\ -q & p & 0 \end{bmatrix} \begin{Bmatrix} u \\ v \\ w \end{Bmatrix} + \frac{g}{W} \begin{Bmatrix} X \\ Y \\ Z \end{Bmatrix}, \tag{1}$$

where X, Y and Z represent the aerodynamic forces along the body axes, g is the the gravitational acceleration and W is the aircraft weight. In a similar way, moment equations are expressed as follows

$$\begin{Bmatrix} \dot{p} \\ \dot{q} \\ \dot{r} \end{Bmatrix} = [I_B]^{-1} \left(\begin{Bmatrix} \mathbb{L} \\ \mathbb{M} \\ \mathbb{N} \end{Bmatrix} - \begin{bmatrix} 0 & -r & q \\ r & 0 & -p \\ -q & p & 0 \end{bmatrix} [I_B] \begin{Bmatrix} p \\ q \\ r \end{Bmatrix} \right), \tag{2}$$

in which $\mathbb{L}$, $\mathbb{M}$ and $\mathbb{N}$ are the aerodynamic moments in body reference frame and $I_B \in \mathbb{R}^{(3,3)}$ is the tensor of inertia.

The Euler angles are defined starting from the kinematic equations

$$\begin{Bmatrix} \dot{\phi} \\ \dot{\theta} \\ \dot{\psi} \end{Bmatrix} = \begin{bmatrix} 1 & \frac{S_\theta}{C_\theta} & \frac{C_\phi S_\theta}{C_\theta} \\ 0 & C_\phi & -S_\phi \\ 0 & \frac{S_\phi}{C_\theta} & \frac{C_\phi}{C_\theta} \end{bmatrix} \begin{Bmatrix} p \\ q \\ r \end{Bmatrix}, \tag{3}$$

where $S_{(\cdot)}$ and $C_{(\cdot)}$ are respectively sine and cosine functions.

Finally, position coordinates in NED reference frame are defined by means of navigation equations

$$\begin{Bmatrix} \dot{X}_N \\ \dot{Y}_E \\ \dot{Z}_D \end{Bmatrix} = \begin{bmatrix} C_\theta \cdot C_\psi & S_\phi \cdot S_\theta \cdot C_\psi - C_\phi \cdot S_\psi & C_\phi \cdot S_\theta \cdot C_\psi + S_\phi \cdot S_\psi \\ C_\theta \cdot S_\psi & S_\phi \cdot S_\theta \cdot S_\psi + C_\phi \cdot C_\psi & C_\phi \cdot S_\theta \cdot S_\psi - S_\phi \cdot C_\psi \\ -S_\theta & S_\phi \cdot C_\theta & C_\phi \cdot C_\theta \end{bmatrix} \begin{Bmatrix} u \\ v \\ w \end{Bmatrix}. \tag{4}$$

B. Flexible Model

The flexible model is based on a Lagrangian approach and considers the wing as a deformable element, while the rest of the aircraft is considered rigid. In order to represent the behavior of a flexible system reducing the model complexity, an appropriate set of generalized coordinates must be chosen. The Galërkin method [15] is used to define the wing bending and torsion as truncated series expansions, in the form

$$\xi_w(x_w, t) = \sum_{j=1}^{N} \Phi_j(x_w)\eta_j^w(t), \tag{5}$$

$$\theta_w(x_w, t) = \sum_{j=1}^{N} \Psi_j(x_w)\zeta_j^w(t), \tag{6}$$

where $\eta_j^w(t)$ and $\zeta_j^w(t)$ are the amplitudes of the structural modes represented by $\Phi_j(x_w)$ and $\Psi_j(x_w)$ shape functions, which should satisfy the physical and geometric boundary conditions of the considered element. The number of structural modes influences the required computational effort.

In this study, we design the flexible model only for the longitudinal motion, so only the symmetric aeroelastic modes affect the aircraft responses. In detail, only the first two symmetric bending modes and the first symmetric torsional mode are considered. According to Eq. (5), wing bending and torsional displacements can be expressed as

$$\xi_w(x_w, t) = \Phi_1(x_w)\eta_1^w(t) + \Phi_2(x_w)\eta_2^w(t), \tag{7}$$

$$\theta_w(x_w, t) = \Psi_1(x_w)\zeta_1^w(t). \tag{8}$$

In this way,the elastic displacements are represented by means of a finite number of generalized coordinates, represented by the bending and torsional modes amplitudes $\eta = [\eta_1, \eta_2, \zeta_1]^T \in \mathbb{R}^3$. Therefore, the complete state vector of the aeroelastic system can be expressed has $\mathrm{x} = [\mathrm{U}, \omega, \Phi, \mathrm{X}, \eta]^{\mathrm{T}} \in \mathbb{R}^{15}$.

Once the appropriates set of coordinates is chosen, the flexible dynamics is derived by means of the Lagrange equations,

$$\frac{d}{dt}\frac{\partial \mathcal{L}}{\partial \dot{q}} - \frac{\partial \mathcal{L}}{\partial q} = Q_q, \tag{9}$$

with q generalized coordinates. Q_q represents the generalized forces and $\mathcal{L}$ is the Lagrangian, defined as

$$\mathcal{L} = \mathcal{T} - \mathcal{U}, \tag{10}$$

with $\mathcal{T}$ and $\mathcal{U}$ respectively kinetic and potential energy.

The kinetic energy of the flexible wing can be expressed as

$$\mathcal{T}_w = \frac{1}{2}\int_0^{l_w} \mu_w \dot{R}_w \cdot \dot{R}_w \, dx_w + \frac{1}{2}\int_0^{l_w} \Omega_w^T j_w \Omega_w \, dx_w. \tag{11}$$

μ_w represents the mass density per unit of length and j_w is the inertial tensor of the wing element. Finally, $\dot{R}_w$ and Ω_w are respectively the linear velocity vector and the angular rate vector, in which wing deflection ξ_w and torsion θ_w are included. In general,

$$\dot{R}_w = V_B + \omega_B \times r_w + \dot{\xi}_w, \tag{12}$$

$$\Omega_w = \omega_B + \dot{\theta}_w \times \hat{\tau}_w + \dot{\xi}'_w. \tag{13}$$

V_B and ω_B are linear and angular rate vectors in body reference frame, r_w is the position of the considered wing element in the wing reference frame and $\hat{\tau}_w$ is the torsion axis. Note that, in the following equation, $\dot{()}$ and $()'$ represent time and space derivatives, respectively. Eqs. (12) and (13) can be rewritten as

$$\dot{R}_w = \begin{Bmatrix} u \\ v \\ w \end{Bmatrix} + \begin{Bmatrix} p \\ q \\ r \end{Bmatrix} \times [C_w]^T \begin{Bmatrix} x_w \\ y_w \\ z_w + \xi_w \end{Bmatrix} + [C_w]^T \begin{Bmatrix} 0 \\ 0 \\ \dot{\xi}_w \end{Bmatrix}, \tag{14}$$

$$\Omega_w = \begin{Bmatrix} p \\ q \\ r \end{Bmatrix} + [C_w]^T \begin{Bmatrix} \dot{\theta}_w \\ 0 \\ 0 \end{Bmatrix} + \begin{Bmatrix} 0 \\ -\dot{\xi}'_w \\ 0 \end{Bmatrix}, \tag{15}$$

where C_w is the transformation matrix between body and wing reference frames. In this work, the wing reference frame has the x_w axis along the wingspan, z_w axis points downwards and the y_w axis to form a right-handed system, as reported in the example in Figure 2. Defining the sweep angle Λ and the dihedral angle Γ of the wing, C_w is

$$C_w = \begin{bmatrix} -\sin\Lambda\cos\Gamma & \cos\Lambda\cos\Gamma & -\sin\Gamma \\ -\cos\Lambda & -\sin\Lambda & 0 \\ -\sin\Lambda\sin\Gamma & \cos\Lambda\sin\Gamma & \cos\Gamma \end{bmatrix}. \tag{16}$$

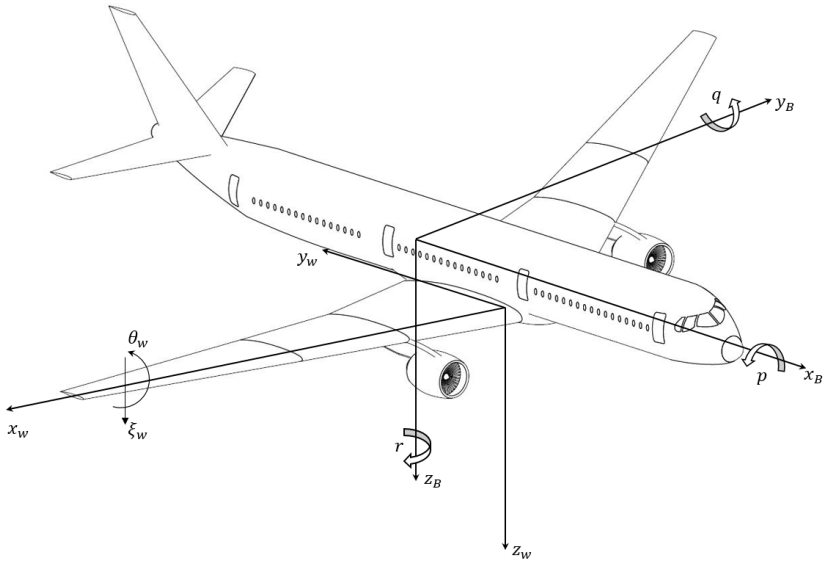

Fig. 2 Reference Frame and Flexible Parameters

The potential energy can be written as the sum of the elastic energy of the system flexible parts and the gravitational potential. In this work, since the wing is the only flexible part, the potential energy can be written as

$$\mathcal{U} = \mathcal{U}_{wb} + \mathcal{U}_{wt} + \mathcal{U}_{wg}. \tag{17}$$

$\mathcal{U}_{wb}$ is the potential energy due to the wing bending, according to the Euler-Bernoulli beam theory, $\mathcal{U}_{wb} = \frac{1}{2}\int_0^{l_w} EI_w(\xi_w'')^2\, dx_w$ and $\mathcal{U}_{wt}$ is the potential energy due to the wing torsion, $\mathcal{U}_{wt} = \frac{1}{2}\int_0^{l_w} EJ_{t,w}(\theta_w')^2\, dx_w$.

Finally, when a wing bending is evaluated, a potential energy due to the change in altitude $\mathcal{U}_{wg}$ should be included, $\mathcal{U}_{wg} = \int_0^{l_w} \mu_w g(\xi_w \cos\theta)\, dx_w$.

Note that both the kinetic and the potential energy are expressed in terms of both rigid and flexible variables. The rigid terms are known and obtained from the equations of motion, while the flexible displacements can be expressed in terms of generalized coordinates by means of the Galërkin method.

The generalized forces Q_q can be defined through the principle of virtual work $\partial W = \sum_{h=1}^{k} F_h \cdot \partial r_h$, where, for the dependant variable r in presence of k external forces, ∂r is the virtual displacement which could be also expressed in terms of the N generalized coordinates. So,

$$\partial W = \sum_{h=1}^{k} F_h \sum_{j=1}^{N} \frac{\partial r_h}{\partial q_j}\partial q_j = \sum_{j=1}^{N}\left(\sum_{h=1}^{k} F_h \frac{\partial r_h}{\partial q_j}\right)\partial q_j = \sum_{j=1}^{N} Q_{q_j}\partial q_j, \tag{18}$$

where

$$Q_{q_j} = \sum_{h=1}^{k} F_h \frac{\partial r_h}{\partial q_j} \quad \text{with} \quad j = 1, ..., N. \tag{19}$$

In this study, the virtual work of each flexible part can be expressed as a function of external forces that act on it (i.e., aerodynamic distributed and concentrated loads) multiplied by the virtual displacements, which are the dependent variables. So, similarly to Eq. (18), for the flexible wing we have

$$\partial W_{w,b} = \int_0^{l_w} f_{Aw}(\alpha_w, x_w)\xi_w(x_w, t)\, dx_w \tag{20}$$

$$\partial W_{w,t} = \int_0^{l_w} M_{Aw}(\alpha_w, x_w)\theta_w(x_w, t),\, dx_w \tag{21}$$

where f_{Aw} and M_{Aw} represent the distributed aerodynamic force and moment generated by the wing. Note that, if the aircraft engine is mounted under the wing, a concentrated load must be considered at the corresponding wing section. In this work, the aerodynamic loads of each section are considered to be dependant only on the angle of attack and its variation due the maneuver and wing deformation, as in [7],

$$f_{Aw} = \frac{1}{2}\rho V^2 S C_{L_\alpha}\alpha_w, \tag{22}$$

$$M_{Aw} = \frac{1}{2}\rho V^2 S C_{L_\alpha}(x_\theta - x_{CA})\alpha_w, \tag{23}$$

where $(x_\theta - x_{CA})$ represents the distance between the torsion axis and the airfoil aerodynamic center, and α_w is given by the sum of aircraft angle of attack α_{WB}, wing twist angle i_w, pitch rate q, bending rate $\dot{\xi}$, torsion angle θ and its time derivative $\dot{\theta}$:

$$\alpha_w \approx \alpha_{WB} + i_w(x_w) - \frac{q}{u}x_F(x_w) + \frac{\dot{\xi}_w(x_w, t)}{u} + \theta_w(x_w, t) + \frac{\dot{\theta}_w(x_w, t)(x_\theta - x_{CA})}{u}, \tag{24}$$

where x_F represents the distance between the aerodynamic centre of the considered section and the aircraft center of gravity in body reference frame.

External aerodynamic force and moment can be written as in [7]

$$f_{Aw}(x) = f_{A_0} + \frac{\partial f_A}{\partial \dot{\xi}_w}\dot{\xi}_w \tag{25}$$

$$M_{Aw}(x) = M_{A_0} + \frac{\partial M_A}{\partial \dot{\theta}_w}\dot{\theta}_w, \tag{26}$$

where the subscript 0 indicates the aerodynamic load generated by the "frozen" configuration and the second term is the increment generated by deformation rates. This approach permits to split the virtual work, expressed for the k-th wing

element as discussed in [7]. The contribution to the virtual work of the "frozen" term generated by aerodynamic force and moment can be simply expressed as

$$\int_0^{l_k} f_{A_0}\delta\xi\, dx_k = \int_0^{l_k} \frac{1}{2}\rho V^2 S c^{(k)} C_{L_\alpha}\left[\alpha_{WB} + \theta_{w,k} - \frac{q}{u}x_F\right]\left(\Phi_1^{(k)}\delta\eta_1 + \Phi_2^{(k)}\delta\eta_2\right) dx_k, \tag{27}$$

$$\int_0^{l_k} M_{A_0}\delta\theta\, dx_k = \int_0^{l_k} \frac{1}{2}\rho V^2 S c^{(k)} C_{L_\alpha}(x_\theta - x_{CA})\left[\alpha_{WB} + \theta_{w,k} - \frac{q}{u}x_F\right]\left(\Psi_1^{(k)}\delta\zeta_1\right) dx_k, \tag{28}$$

in which $c^{(k)}$ is the chord of the k-th wing element.

The second term of Eq. (25) and (26), generated by deformation rates, can be expressed in terms of Rayleigh dissipation function $\mathcal{F}$ as deeply discussed in [3, 6, 7]. The Rayleigh dissipation function is used to represent the viscous damping forces by means of a single scalar. The viscous damping is proportional to the generalized velocities $\dot{q}_j$ and is one of the most important non-conservative forces acting on an aerodynamic surface. Starting from this definition of the external forces, the Lagrange equation could be written as

$$\frac{d}{dt}\frac{\partial\mathcal{L}}{\partial\dot{q}} - \frac{\partial\mathcal{L}}{\partial q} + \frac{\partial\mathcal{F}}{\partial\dot{q}} = Q_{q_0}, \tag{29}$$

where Q_{q_0} represents the generalized forces generated by the "frozen" configuration. In this work, when referring to the generalized forces Q_q both "frozen" and viscous damping forces are considered. The terms of the Rayleigh's dissipation function relative to wing bending $\mathcal{F}_b$ and torsion $\mathcal{F}_t$, are defined as

$$\mathcal{F}_b^{(k)} = \dot{\eta}^T C_b^{(k)}\dot{\eta} = \{\dot{\eta}_1\ \dot{\eta}_2\}\left[C_b^{(k)}\right]\begin{Bmatrix}\dot{\eta}_1\\ \dot{\eta}_2,\end{Bmatrix} \tag{30}$$

$$\mathcal{F}_t^{(k)} = \dot{\zeta}^T C_t^{(k)}\dot{\zeta} = \dot{\zeta}_1\left[C_t^{(k)}\right]\dot{\zeta}_1. \tag{31}$$

$C_b^{(k)}$ matrix becomes

$$\begin{bmatrix} \frac{1}{2}\int_0^{l_k} q_d S c^{(k)} C_{L_\alpha}\left[\frac{1}{u}\right]\Phi_1^2(x_k)\, dx_k & \frac{1}{2}\int_0^{l_k} q_d S c^{(k)} C_{L_\alpha}\left[\frac{1}{u}\right]\Phi_1(x_k)\Phi_2(x_k)\, dx_k \\ \frac{1}{2}\int_0^{l_k} q_d S c^{(k)} C_{L_\alpha}\left[\frac{1}{u}\right]\Phi_2(x_k)\Phi_1(x_k)\, dx_k & \frac{1}{2}\int_0^{l_k} q_d S c^{(k)} C_{L_\alpha}\left[\frac{1}{u}\right]\Phi_2^2(x_k)\, dx_k \end{bmatrix}, \tag{32}$$

where $q_d = \frac{1}{2}\rho V^2$ is the dynamic pressure. For the torsional mode,

$$C_t^{(k)} = \int_0^{l_k} \frac{1}{2}\rho V^2 S c^{(k)} C_{L_\alpha}(x_\theta - x_{CA})\left[\frac{(x_\theta - x_{CA})}{u}\right]\Psi_1^2(x_k)\, dx_k. \tag{33}$$

Finally, the virtual work of Eq. (18) can be rewritten as

$$\delta W = Q_{q_1}\delta q_1 + ... + Q_{q_n}\delta q_n = Q_{\eta_1}\delta\eta_1 + Q_{\eta_2}\delta\eta_2 + Q_{\zeta_1}\delta\zeta_1. \tag{34}$$

Since we are considering only two bending modes and one torsional mode, the complete system is the following

$$\begin{cases} \frac{d}{dt}\frac{\partial\mathcal{L}}{\partial\dot{\eta}_1} - \frac{\partial\mathcal{L}}{\partial\eta_1} = Q_{\eta_1} \\ \frac{d}{dt}\frac{\partial\mathcal{L}}{\partial\dot{\eta}_2} - \frac{\partial\mathcal{L}}{\partial\eta_2} = Q_{\eta_2} \\ \frac{d}{dt}\frac{\partial\mathcal{L}}{\partial\dot{\zeta}_1} - \frac{\partial\mathcal{L}}{\partial\zeta_1} = Q_{\zeta_1} \end{cases}, \tag{35}$$

which can be organized as a second order system (MCK form)

$$M\ddot{q} + C\dot{q} + Kq = f_q. \tag{36}$$

C. Linearized Mathematical Model

For the evaluation of the controller gains and parameters, for both selected controllers, the rigid aircraft is defined as a Linear-Time- Inavariant (LTI) system as follows

$$\dot{x} = Ax + Bu, \tag{37}$$

where $A \in \mathbb{R}^{n,n}$ is the state matrix, $x \in \mathbb{R}^n$ is the state vector, $B \in \mathbb{R}^{n,m}$ is the control matrix and $u \in \mathbb{R}^m$ is the control vector. Since only the longitudinal dynamics are considered in the aircraft model, the state vector is composed as $x = \{u, w, q, \theta\}^T$ with $n = 4$, while the control vector contains only elevator and aileron deflections, neglecting throttle effects, $u = \{\delta_e, \delta_a\}^T$ (i.e. $m = 2$).

In order to obtain a state-space definition of the system which can be used in the controllers design, matrices A and B are written in a non-dimensional form. Starting from non-dimensional forces and moments, we have $\hat{F}_i = \dfrac{F_i}{\frac{1}{2}\rho V_0^2 S}$ and $\hat{M}_i = \dfrac{M_i}{\frac{1}{2}\rho V_0^2 S\bar{c}}$, in which the superscript ($\hat{}$) indicates the non-dimensional form of the variable. The aircraft mass and the inertial tensor can be adimensionalized as $\hat{m} = \dfrac{2m}{\rho S\bar{c}}$ and $\hat{I}_y = \dfrac{I_y}{\rho S\left(\frac{\bar{c}}{2}\right)^3}$. Finally, the time derivative in non dimensional form can be written as $\dfrac{d}{dt} = \dfrac{2V_0}{\bar{c}}$.

Starting from the previous definitions, the non-dimensional form of the states is $\hat{x} = \left\{\frac{u}{V_0}, \frac{w}{V_0}, q\frac{\bar{c}}{2V_0}, \theta\right\}^T = \{\hat{u}, \alpha, \hat{q}, \theta\}^T$. The state and control matrices become, respectively

$$A = \begin{bmatrix} -\dfrac{3C_{D_0}}{2\hat{m}} & \dfrac{C_{L_0} - C_{D_\alpha}}{2\hat{m}} & 0 & -\dfrac{C_{W_e}}{2\hat{m}} \\ -\dfrac{C_{L_0}}{2\hat{m} + C_{L_{\dot{\alpha}}}} & -\dfrac{C_{L_\alpha} + C_{D_0}}{2\hat{m} + C_{L_{\dot{\alpha}}}} & \dfrac{2\hat{m}}{2\hat{m} + C_{L_{\dot{\alpha}}}} & 0 \\ \dfrac{-C_{M_{\dot{\alpha}}}\dfrac{2C_{L_0}}{2\hat{m} + C_{L_{\dot{\alpha}}}}}{\hat{I}_y} & \dfrac{C_{M_\alpha} - C_{M_{\dot{\alpha}}}\dfrac{C_{L_\alpha} + C_{D_0}}{2\hat{m} + C_{L_{\dot{\alpha}}}}}{\hat{I}_y} & \dfrac{C_{M_q} - C_{M_{\dot{\alpha}}}\dfrac{2\hat{m}}{2\hat{m} + C_{L_{\dot{\alpha}}}}}{\hat{I}_y} & 0 \\ 0 & 0 & 1 & 0 \end{bmatrix}, \tag{38}$$

$$B = \begin{bmatrix} 0 & 0 \\ -\dfrac{C_{L_{\delta_e}}}{2\hat{m} + C_{L_{\dot{\alpha}}}} & -\dfrac{C_{L_{\delta_a}}}{2\hat{m} + C_{L_{\dot{\alpha}}}} \\ \dfrac{C_{M_{\delta_e}}}{\hat{I}_y} & \dfrac{C_{M_{\delta_a}}}{\hat{I}_y} \\ 0 & 0 \end{bmatrix}, \tag{39}$$

in which the derivatives $C_{D_\alpha} = \dfrac{2C_{L_\alpha}}{\pi e\frac{b^2}{S}}C_{L_0}$ and $C_{W_e} = \dfrac{mg}{\frac{1}{2}\rho V_0^2 S}$. All the other derivatives are defined in [14] and in Table 2.

D. Gust Models

As stated before, both discrete and continuous gust models are defined as aircraft perturbation. In both considered model, a gust velocity profile is added to the linear speed components.

The discrete gust model, as in CS 25 regulation [13], consists in a "1 − cos" pulse

$$U_g = \begin{cases} \dfrac{U_{ds}}{2}\left[1 - \cos\left(\dfrac{\pi s}{H}\right)\right] & 0 < s \leq 2H \\ 0 & s > 2H \end{cases}, \tag{40}$$

where s represents the distance penetrated into the gust, H is the gust gradient, between 9 m and 107 m, U_{ds} is the gust velocity in equivalent airspeed,

$$U_{ds} = U_{\text{ref}} F_g \left(\frac{H}{107}\right)^{\frac{1}{6}}. \tag{41}$$

U_{ref} represents the reference gust velocity in equivalent airspeed, indicated by CS 25 regulation as a function of altitude for a gust gradient H of 107 m. Finally, F_g represents the flight profile alleviation factor. and is minimum at sea level, linearly increasing to 1 at the certified maximum altitude.

The "1 − cos" model is simple and particularly useful to simulate large loads acting on the wing surface. However, to represent continuous and irregular nature of the atmospheric turbulence, a continuous gust model, based on von Kármán turbulence model, is proposed. This model defines the linear and angular velocity components of the continuous gust as a stochastic process and specify the Power Spectral Density (PSD) of each component by means of mathematical expressions [11]. For example, the power spectral density of the vertical component of the gust velocity w_g is expressed as

$$\Phi_w(\omega) = \frac{2\sigma_w^2 L_w}{\pi V} \cdot \frac{1 + \frac{8}{3}\left(2.678 L_w \frac{\omega}{V}\right)^2}{\left[1 + \left(2.678 L_w \frac{\omega}{V}\right)^2\right]^{\frac{11}{6}}}, \tag{42}$$

where V is the aircraft speed, σ_w defines the turbulence intensity, which is the Root Mean Square (RMS) gust component, and L_w represents the turbulence scale length. Both turbulence intensity σ and scale length L values depend on altitude and flight conditions, as indicated in the design procedures reported on [12].

The gust velocity time history is obtained by passing a band limited white noise through a forming filter derived from the gust PSD [16]. This leads to an output signal with the same PSD of the chosen model, which can be used directly as wind disturbance inside the rigid equations of motion.

III. Wing Load Evaluation

The rigid model dynamics influences the flexible wing dynamics, in terms of bending, torsion and their relative rates, as defined before. After a perturbation, the dynamic wing loads are changed, so load evaluation is important in both aircraft structural analysis, which is largely performed via Finite Element Method (FEM) methods, and in control system design, especially for Gust Load Alleviation (GLA) purposes.

In the proposed models, *a priori* FEM analysis of the flexible structure is performed to define shape functions and Young's modulus of each wing sections. In this work, two approaches for gust load evaluation are introduced and compared: (i) one is directly related to the flexible model in the MCK form,and (ii) one is related to the strip theory [17]. The first method is more accurate than the second, in which some approximations and simplifications are introduced. Moreover, for control law synthesis, the second method is more efficient from the computational point of view.

A. MCK Load Formulation

Since an external gust perturbs the aircraft, the matrix form of the Lagrange equation system (Eq. (36)) can be rewritten as

$$M\ddot{q} + C\dot{q} + Kq = f_{q_0} + f_g, \tag{43}$$

where f_g represents the vector of elastic loads generated by the external perturbation in terms of generalized coordinates. This component appears in the equation since external aerodynamic forces can be expressed as sum of the load generated by the current values of transport and deformation variables ("frozen" configuration) and the load increment generated by the deformation rates. The term f_g represents this load increment over the "frozen" loads of the trim conditions f_{q_0}. In practice, f_g represents the dynamic load terms given by the Rayleigh dissipation functions. Starting from the previous equations, the elastic loads can be easily determined in terms of generalized coordinates. The gust force and moment have to be properly defined in a wing reference frame, as

$$f_{a_g}^{(k)} = f_{g_{\eta_1}} \Phi_1^{(k)} + f_{g_{\eta_2}} \Phi_2^{(k)}, \tag{44}$$

$$M_{a_g}^{(k)} = f_{g_{\zeta_1}} \Psi_1^{(k)}. \tag{45}$$

The terms $f_{a_g}^{(k)}$ and $M_{a_g}^{(k)}$ represent the aerodynamic force and moment generated by the wing deformation on the k-th wing element, respectively.

These loads are expressed in terms of the aerodynamic chord of the considered section and thus can be seen as distributed loads over the wing span. Note that the dynamic loads are defined in wing sections. In detail, the critical section is the wing root, so the control objective is to reduce the loads in this wing section. So, the bending moment generated by the wing deflection at the wing root can be expressed as follows

$$M_{\text{bending}} = M_{y_w} = \sum_{k=1}^{N} \int_0^{x^{(k)}} f_{a_g}^{(k)} x_w^{(k)} \, dx = \sum_{k=1}^{N} f_{a_g}^{(k)} \frac{x_w^{2(k)}}{2}. \tag{46}$$

In a similar way, the torsional moment can be calculated at the wing root as follows

$$M_{\text{torsion}} = M_{x_w} = \sum_{k=1}^{N} M_{a_g}^{(k)} x_w^{(k)}. \tag{47}$$

Following this approach, the wing loads, in terms of wing bending and torsion moment, can be evaluated, starting directly from the MCK form. This is convenient if a model of the flexible dynamics is available, which requires several structural terms, from *a priori* structural analysis. However, if only information in terms of deformations and relative deformation rates are available, the MCK method results difficult to apply, and therefore an alternative approach is proposed.

B. Strip Theory Load Formulation

Neglecting 3D effects associated with finite elongation wing, the aerodynamic loads can be expressed in terms of local angle of attack variation of every considered wing section. This angle of attack can be expressed in terms of rigid and flexible variables and, in the hypothesis of small perturbations, can be expressed as in Eq. (24).

Note that the spatial derivative of the wing deflection $\xi_w^{'}$ does not influence the local angle of attack, but it generates a small rotation of the lift vector around the y_w axis of the wing reference frame. However, in this case, since the deformations are small, the effect of this rotation can be neglected.

Therefore, knowing α_w and C_{L_α} of the considered wing element, the lift coefficient C_L can be evaluated

$$C_L(\alpha_w, x_w) = C_{L_\alpha}(x_w)\alpha_w(x_w), \tag{48}$$

and the drag coefficient C_D by the following quadratic relation

$$C_D(\alpha_w, x_w) = C_{D_0} + k \left(C_L(\alpha_w, x_w)\right)^2, \tag{49}$$

with $k = \frac{1}{\pi \frac{b^2}{S} e}$,in which e is the Ostwald factor, b is the wing span and S is the wing surface. The force coefficient C_Z of each wing section is

$$C_Z(\alpha_w, x_w) = -C_L(\alpha_w, x_w)\cos\alpha_w - C_D(\alpha_w, x_w)\sin\alpha_w. \tag{50}$$

Finally, the aerodynamic force and moment on each wing section are

$$f_{Aw} = \frac{1}{2}\rho V^2 c(x_w) C_Z(\alpha_w, x_w), \tag{51}$$

and

$$M_{Aw} = \frac{1}{2}\rho V^2 c(x_w) C_Z(\alpha_w, x_w)(x_\theta - x_{CA}). \tag{52}$$

These loads are expressed in terms of the aerodynamic chord of the considered section and thus they can be seen as distributed loads over the wing span. Therefore bending and torsion moments at the wing root can be expressed by means of Eq. (46) and Eq. (47), as in the MCK formulation.

IV. Control System Design

The objective of the proposed control strategies is to reduce the wing deformations, and deformation rates, in order to reduce the dynamic loads acting on the wing, when a perturbation occurs.

However, applying an effective controller directly in the flexible variables is not simple and requires a large amount of data concerning the flexible structure. For this reason, the control strategies are applied on the rigid aircraft dynamics, in order to *indirectly* reduce the generated dynamic loads.

The first approach presented in this work consists on a Linear Quadratic Regulator (LQR) [18], applied to both elevator and symmetric aileron deflections. The second approach is the $\mathcal{L}_1$ adaptive controller [8] for the gust alleviation, as developed in [10]. The advantage of this controller consists in its capacity to adapt to the uncertainties deriving from the weight and flight condition variation. Note that for gust load alleviation two control surfaces are considered: (i) the elevator surface, to alleviate the loads generated by perturbation and by maneuvers, and (i) the symmetric aileron deflection, only to decrease the perturbation loads (longitudinal plane). The anti-symmetric aileron deflection is not considered in this work, since we are only analyzing the longitudinal motion of the aircraft.

A. Linear Quadratic Regulator

In order to define the LQR gain, the system should be linearized, as specified in Section II.C. A standard continuous time-invariant state space is formulated, as in [10], and the matrices of the system are in Section II.C and Equations 38 and 39. As well known, the design of an LQR controller consists in generating a control input equal to $u = -Kx$, with x state vector. The static gain $K = R^{-1}B^T P$ is obtained by the solution P of the associated Algebraic Riccati Equation (ARE).

$$PA + A^T P - PBR^{-1}B^T P + Q = 0 \tag{53}$$

Moreover, two weighting matrices Q and R are selected including limits of the states (Q) and of the actuation dynamics (R). The corresponding control action minimizes the classical quadratic cost function

$$J(x,u) = \int_0^\infty (x^T Qx + u^T Ru)\mathrm{dt}. \tag{54}$$

The obtained state-feedback gain, by minimizing the longitudinal rigid variables, indirectly reduces the dynamic loads generated by the wing deformation. Both elevator and symmetric-aileron deflections are considered as control inputs. The state variables are described in Section II.C.

B. $\mathcal{L}_1$ Adaptive Controller

The choice of the $\mathcal{L}_1$ adaptive controller for the feedback aircraft control is motivated by the high level of model uncertainty (by the variations of the mass and flight conditions) and by high oscillations in the model responses (by state- and time-dependent nonlinearities). This controller is composed by three main blocks: (i) the adaptive law, (ii) the state predictor, and (iii) the control law, as in Figure 3.

The state predictor, which is designed to reproduce the actual plant structure and to specify the desired behavior of the closed-loop system, generates a prediction of the system state. Even if a complete rigid-flexible model is considered, the controller state predictor (for Multi-Input-Multi-Output (MIMO) and Single-Input-Single-Output (SISO) cases) reproduces only the rigid dynamics and the flexible components are *indirectly* controlled by these variables. Moreover, the linearized model in Section II.C is used as reference. The scope of this simplified design is to verify whether or not the overall system can be controlled by using the rigid states of the aircraft [19].

An important feature of the $\mathcal{L}_1$ controller is that the error between the closed loop system and the reference controller can be uniformly bounded by a constant proportional to the adaptation sampling rate. Another important key aspect is that this controller defines the control signal as the output of a low-pass filter to guarantee that the control signal stays in the low-frequency range. The low-pass filter for this application is designed with a mixed deterministic and randomized approach as described in [20]. The above described controller is designed to control the general linear system of Eq. (37) which, considering uncertainties, can be rewritten as

$$\begin{aligned} \dot{x}(t) &= A_m x(t) + B_m(\omega u(t) + f_1(x(t), z(t), t)) + B_{um} f_2(x(t), z(t), t),\ x(0) = x_0, \\ z(t) &= g_o(x_z(t), t),\ \dot{x}_z(t) = g(x_z(t), x(t), t),\ x_z(0) = x_{z0}, \\ y(t) &= Cx(t). \end{aligned} \tag{55}$$

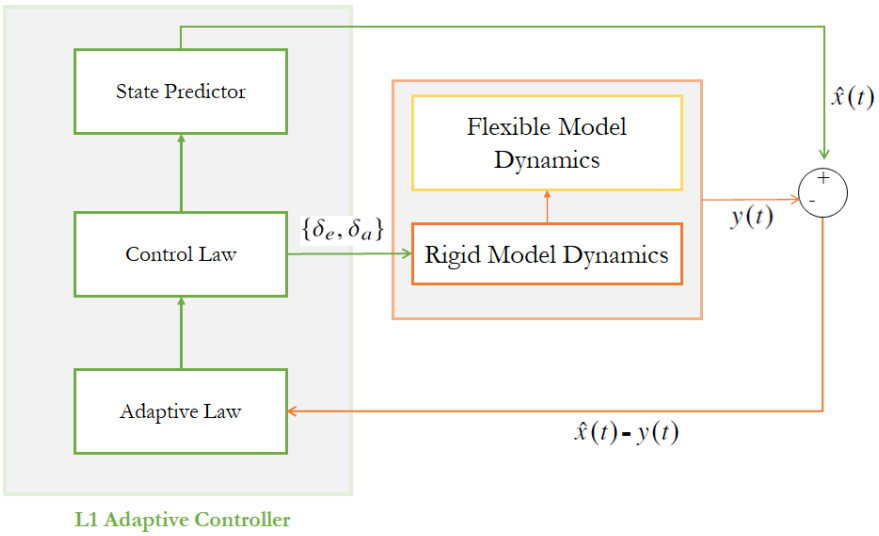

Fig. 3 L1 Adaptive Controller Scheme

The matrix $A_m \in \mathbb{R}^{n,n}$ is Hurwitz and specifies the desired dynamics of the closed-loop system, $B_m \in \mathbb{R}^{n,m}$ and $C \in \mathbb{R}^{m,n}$ are known constant matrices. $B_{um} \in \mathbb{R}^{n,(n-m)}$ is a constant matrix such that $B_m^T B_{um} = 0$ and the rank of $B = [B_m\ B_{um}]$ is n. Compared to system (37), the system (55) includes $\omega \in R^{m\times m}$ the unknown frequency gain matrix, $z(t)$ and $x_z(t)$ respectively the output and state vector of internal unmodeled dynamics and the unknown nonlinear functions $g(\cdot)$ and $g_0(\cdot)$. In the analyzed $\mathcal{L}_1$ control system, $B_m = B$ and two variables are controlled by two control inputs.

The state predictor is defined as

$$\dot{\hat{x}}(t) = A_m\hat{x}(t) + B_m(\omega_0 u(t) + \hat{\sigma}_1(t)) + B_{um}\hat{\sigma}_2(t),\ \hat{x}(0) = x_0$$

where the adaptive vectors $\hat{\sigma}_1(t) \in R^m$ and $\hat{\sigma}_2(t) \in R^{n-m}$, with ω_0 a candidate nominal frequency, are

$$\begin{bmatrix} \hat{\sigma}_1(t) \\ \hat{\sigma}_2(t) \end{bmatrix} = -\begin{bmatrix} \mathbb{I}_m & 0 \\ 0 & \mathbb{I}_{n-m} \end{bmatrix} B^{-1}\Phi^{-1}(T_s)\mu(iT_s), \tag{56}$$

for $i = 0, 1, 2, \ldots$, and $t \in [iT_s, (i+1)T_s]$, where $T_s > 0$ is the adaptation sampling time associated with the sampling rate of the Fligh Control System (FCS) computer. In Equation (56), we also have

$$\Phi(T_s) = A_m^{-1}(e^{A_m T_s} - \mathbb{I}_n),\ \in R^{n\times n}$$
$$\mu(iT_s) = e^{A_m T_s}\tilde{x}(iT_s),$$

where $\tilde{x}(t) = \hat{x}(t) - x(t)$ is the error between the system state and the predicted state.

A prefilter Kg, chosen as the constant matrix $K_g = -(CA_m^{-1}B_m)^{-1}$, is defined to achieve decoupling among the signals.

For all the details of the $\mathcal{L}_1$ Adaptive controller refer to [21].

V. Simulation Results

In order to analyze the time response of the flexible aircraft, when a gust perturbation occurs, a simulation model is implemented on Matlab/Simulink® software. The characteristics of the aircraft, considered in this study, are in Table 1. A maximum deflection of ±10 deg for gust load alleviation is considered.

Both gust profiles are considered in simulations. A "1 − cos" vertical discrete gust as described in Eq. (40), with $H = 26$ m and $U_{\text{ref}} = 17.07$ m/s, is shown in Figure 4. The second perturbation, based on von Karman continuous vertical gust, is shown in Figure 5. Since we are analyzing only the cruise phase, the turbulence scale length L is set to

Table 1 Aircraft characteristics

Wing Geometry & Aircraft Mass	
Wing Span	29 m
Mean Aerodynamic Chord	2.5 m
Wing Surface	73.2 m^2
Aircraft Mass	20100 kg
Mach Number	0.3
Aircraft Altitude	20000 ft

Table 2 Aerodynamic Derivatives of the transport aircraft

Parameter [rad^{-1}]	Value
C_{D_0}	0.0346
C_{L_0}	0.3064
$C_{L\alpha}$	6.4671
$C_{m\alpha}$	−1.5561
$C_{L_{\dot{\alpha}}}$	3.752
$C_{m_{\dot{\alpha}}}$	−22.75
C_{mq}	−70.48
$C_{L_{\delta e}}$	0.4680
$C_{M_{\delta e}}$	−0.695
$C_{L_{\delta a}}$	−2.85
$C_{M_{\delta a}}$	−0.1960

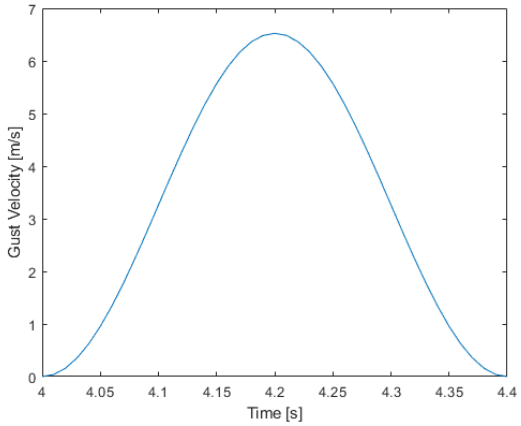

Fig. 4 "1 − cos" Gust Profile

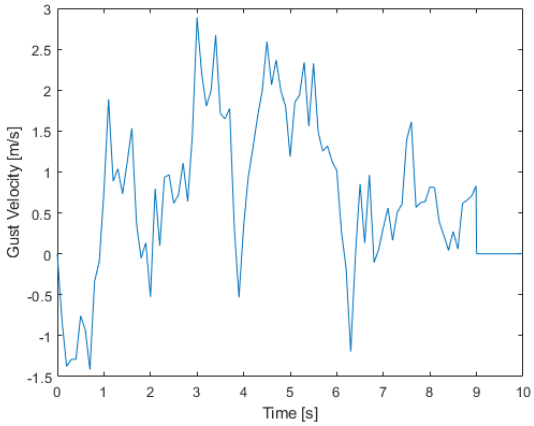

Fig. 5 Continuous von Kármán Gust Profile

2500 ft. The turbulence intensity σ (RMS) $[m/s]$ is set to "moderate" which corresponds to a probability of exceedance of $10^{-3}c/h$.

The data obtained form the flexible model is then used to evaluate the dynamic loads in terms of wing-root bending and torsional moment, by means of MCK formulation, since it is more accurate. As stated before, these dynamics loads can be reduced acting on the aircraft response and, thus, on the wing deformations. In the following section, the results

in terms of load alleviation obtained with an LQR control system and an $\mathcal{L}_1$ controller are shown.

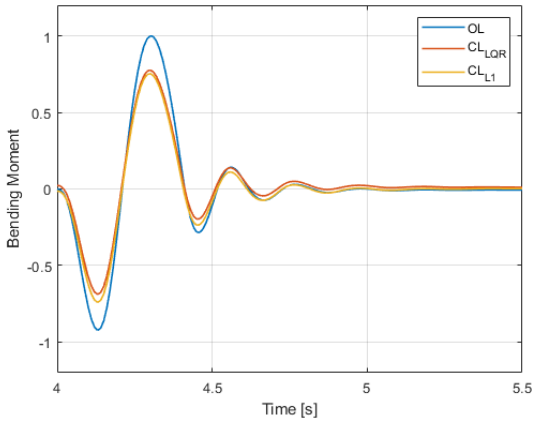

Fig. 6 Open Loop Vs. Closed Loop - Bending Moment - "1 − cos" Discrete Gust

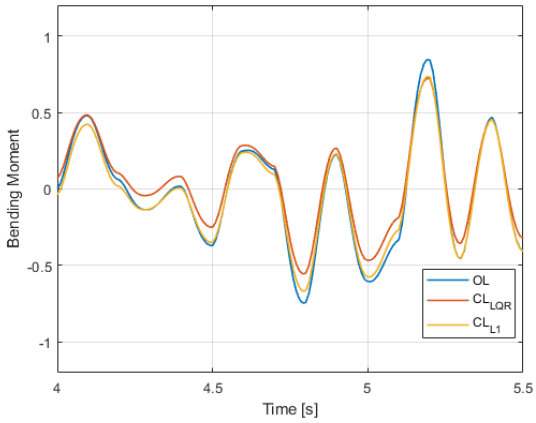

Fig. 7 Open Loop Vs. Closed Loop - Bending Moment - von Karman Gust

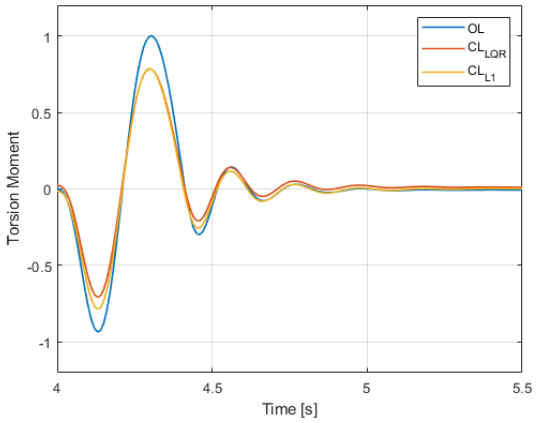

Fig. 8 Open Loop Vs. Closed Loop - Torsional Moment - "1 − cos" Discrete Gust

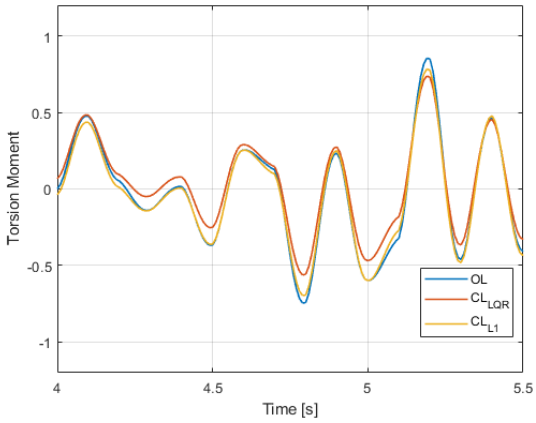

Fig. 9 Open Loop Vs. Closed Loop - Torsional Moment - von Karman Gust

Figures 6 and 8 show the comparison between open- loop and closed-loop loads after a discrete gust occurs, while Figures 7 and 9 show the alleviation, after a von Karman continuous gust.

An effective load reduction with both controllers can be observed, both in terms of bending and torsional moments. For the LQR control system, the reduction at the maximum peak for the discrete "1 − cos" gust is about 22% for the bending moment and about 21% for the torsional moment. The $\mathcal{L}_1$ reaches similar results, with a reduction at the maximum peak of about 23% for the bending moment and about 21% for the torsional moment.

The results obtained with the LQR controller when a von Karman moderate turbulence is considered, although the load reduction is clearly visible, are less consistent, compared with the discrete gust. This is mainly due to the rapid changes in velocity direction and to the small peak of a continuous gust. However, the maximum reduction is of about 26% for the bending moment and 25% for the torsional moment. We can observe an average reduction of about 15% on the overall response. On the other hand, the $\mathcal{L}_1$ controller reaches more consistent results compared with the LQR system on both bending and torsional moments. Although the alleviation is lower than the LQR on some peaks, the $\mathcal{L}_1$ controller never increases the load compared to the open-loop response, self adapting to the rapid gust velocity changes. Overall the $\mathcal{L}_1$ adaptive controller is more reliable than the LQR controller in turbulent gust scenarios.

Different mass and inertial configurations are considered to show the effectiveness of the $\mathcal{L}_1$ adaptive controller. A comparison with the LQR control system is also performed. Both tests are conduced on the "1 − cos" discrete gust.

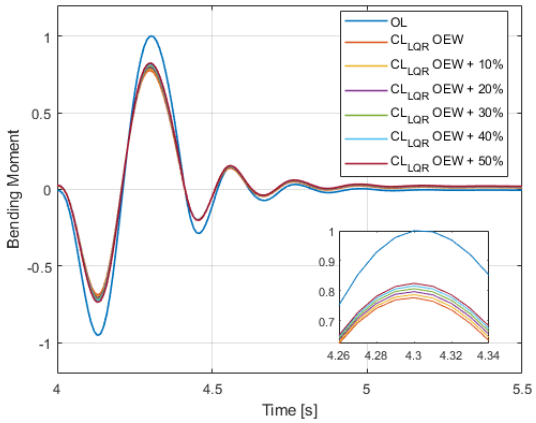

Fig. 10 LQR Alleviation on Bending Moment for a Gradual Mass Increase

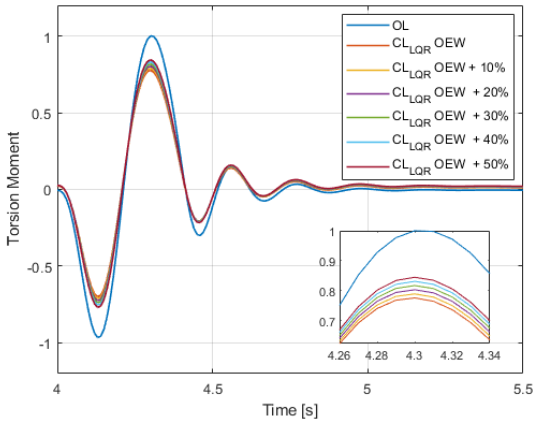

Fig. 11 LQR Alleviation on Torsional Moment for a Gradual Mass Increase

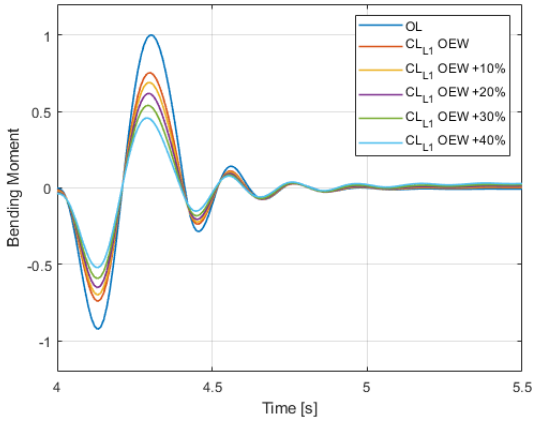

Fig. 12 L1 Alleviation on Bending Moment for a Gradual Mass Increase

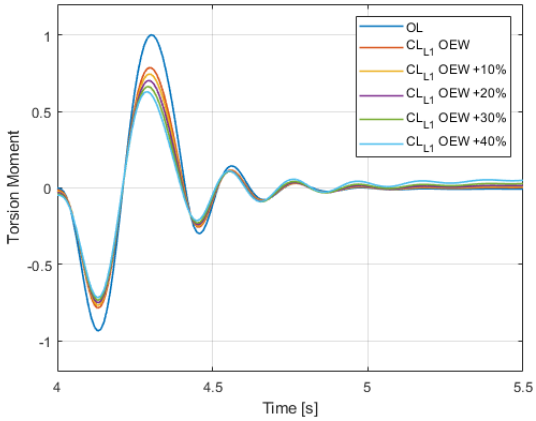

Fig. 13 L1 Alleviation on Torsional Moment for a Gradual Mass Increase

Results of these tests are shown in Figures 10 and 11 for the LQR controller and in Figures 12 and 13 for the $\mathcal{L}_1$ controller. The LQR alleviation gradually decreases with the mass increase, loosing 6% of bending moment reduction and about 8% of torsional moment reduction at the +50% mass increase from the nominal OEW mass condition. As clearly described in [22], the LQR control system is not robust, but it is able to handle variations on the configurations of about 15%. The $\mathcal{L}_1$ controller, on the other hand, shows an increase of load reduction with the mass and inertial properties increase. The aircraft poles become less stable with the mass increase, thus raising the "distance" between the plant dynamics and the desired dynamics specified by A_m matrix. For this reason the reduction of both bending and torsional moments increases, while requiring a greater control effort than the nominal configuration.

VI. Conclusions

A framework for dynamic load evaluation of low-order model of a flexible aircraft is proposed. A mixed Newtonian-Lagrangian approach for the longitudinal model definition is derived, to be easily implemented for real-time simulations. The wing loads are evaluated considering an MCK fomulation, including the definition of the generalized coordinates in a wing reference frame. The dynamic loads due to a gust disturbance are alleviated with an $\mathcal{L}_1$ Adaptive control system and a comparison with a Linear Quadratic Regulator is also proposed. The $\mathcal{L}_1$ controller is able to reduce the dynamic loads, even with a variation of flight conditions and of the mass and inertia properties.

References

[1] Song, S., Whidborne, J. F., Lone, M., and Molina-Cristobal, A., "Multi-Objective Optimal Longitudinal Flight Control System Design for Large Flexible Transport Aircraft," *2018 UKACC 12th International Conference on Control (CONTROL)*, 2018, pp. 81–86.

[2] Chang, C.-S., Hodges, D. H., and Patil, M. J., "Flight Dynamics of Highly Flexible Aircraft," *Journal of Aircraft*, Vol. 45, No. 2, 2008, pp. 538–545. https://doi.org/10.2514/1.30890, URL https://arc.aiaa.org/doi/10.2514/1.30890.

[3] Junkins, J. L., and Kim, Y., *Introduction to dynamics and control of flexible structures*, AIAA education series, American Institute of Aeronautics and Astronautics, Washington, D.C, 1993.

[4] Dowell, E. H., *A Modern Course in Aeroelasticity*, Springer International Publishing, Cham, 2015.

[5] Milne, R., *Dynamics of the Deformable Aeroplane*, Her Majesty's Stationery Office Reports and Memoranda Rept. 3345, Queen Mary College, London, 1964.

[6] Meirovitch, L., and Tuzcu, I., "Unified Theory for the Dynamics and Control of Maneuvering Flexible Aircraft," *AIAA Journal*, Vol. 42, No. 4, 2004, pp. 714–727.

[7] Avanzini, G., Capello, E., and Piacenza, I. A., "Mixed Newtonian–Lagrangian Approach for the Analysis of Flexible Aircraft Dynamics," *Journal of Aircraft*, Vol. 51, No. 5, 2014, pp. 1410–1421.

[8] Naira Hovakimyan, C. C., *L1 Adaptive Control Theory: Guaranteed Robustness with Fast Adaptation (Advances in Design and Control)*, Advances in Design and Control 21, Society for Industrial Applied Mathematics,U.S., 2010.

[9] Avanzini, G., Capello, E., Piacenza, I., Quagliotti, F., Hovakimyan, N., and Xargay, E., "L1 adaptive control of flexible aircraft: preliminary results," *AIAA Atmospheric Flight Mechanics Conference*, 2010, p. 7501.

[10] Capello, E., Guglieri, G., and Quagliotti, F., "A Comprehensive Robust Adaptive Controller for Gust Load Alleviation," *The Scientific World Journal*, Vol. 2014, 2014, pp. 1–12. https://doi.org/10.1155/2014/609027.

[11] Hoblit, F. M., *Gust loads on aircraft: concepts and applications*, AIAA education series, American Institute of Aeronautics and Astronautics, Washington, D.C, 1988.

[12] Department of Defense, U. S., "Flying Qualities of Piloted Aircraft - U.S. Military Handbook MIL-HDBK-1797," , Dec. 1997.

[13] EASA, "Certification Specifications and Acceptable Means of Compliance for Large Aeroplanes CS-25, European Aviation Safety Agency," , 2015.

[14] Etkin, B., *Dynamics of atmospheric flight*, Dover Publications, Mineola, N.Y., 2005.

[15] Meirovitch, L., *Principles and techniques of vibrations*, Prentice Hall, Upper Saddle River, N.J, 1997.

[16] MATLAB Aerospace Blockset Documentations, *Von Karman Wind Turbulence Model (Continuous)*, The MathWorks, Inc., Natick, Massachusetts, 2019. Available on: https://it.mathworks.com/help/aeroblks/vonkarmanwindturbulencemodelcontinuous.html.

[17] Megson, T., *Aircraft Structures for Engineering Students*, 2017. https://doi.org/10.1016/C2009-0-61214-9.

[18] Zhou, K., Doyle, J. C., and Glover, K., *Robust and optimal control*, Prentice Hall, Upper Saddle River, N.J, 1996.

[19] Avanzini, G., Capello, E., Piacenza, I., Quagliotti, F., Hovakimyan, N., and Xargay, E., "L1 adaptive control of flexible aircraft: preliminary results," *AIAA Atmospheric Flight Mechanics Conference*, 2010, p. 7501.

[20] Capello, E., Quagliotti, F., and Tempo, R., "Randomized approaches for control of quadrotor uavs," *Journal of Intelligent & Robotic Systems*, Vol. 73, No. 1-4, 2014, pp. 157–173.

[21] Hovakimyan, N., and Cao, C., *L1 Adaptive Control Theory: Guaranteed Robustness with Fast Adaptation*, Society for Industrial and Applied Mathematics, USA, 2010.

[22] Polyak, B., and Tempo, R., "Probabilistic robust design with linear quadratic regulators," *Systems Control Letters*, Vol. 43, No. 5, 2001, pp. 343 – 353. https://doi.org/https://doi.org/10.1016/S0167-6911(01)00117-7, URL http://www.sciencedirect.com/science/article/pii/S0167691101001177.